INSTABILITY OF HOMOGENEOUS VELOCITY DISTRIBUTION IN AN INDUCTION-TYPE MHD MACHINE

A. Gailitis and O. Lielausis

UDC 538.4:621.313.39

A cylindrical MHD machine is investigated in the regimes in which the magnetic field gets considerably lowered by the currents induced in the fluid. The machine is regarded as a combination of many elementary machines connected in parallel hydraulically and in series electrically. It is shown that in a number of cases the homogeneous flow is unstable. The operating cross section is then divided into several zones with significantly different velocities. The conditions of instability are derived. The consequences of the multivelocity flow are demonstrated by the computation of the p(Q) characteristics as an example. The characteristics of hydraulically parallel operation of two independent machines are investigated in detail. The parallel combination of two narrow machines is put forward as an elementary model of the phenomena occurring inside a wide machine.

The traditional theory of induction-type MHD machines assumes identical velocity V of the fluid over the entire cross section of the operating channel S. The total discharge Q = VS as well as the distribution of the electromagnetic forces $f_{em}(\mathbf{r}, V)$ over the volume of the channel S× L are determined on this basis. The pressure P developed by the machine is calculated by dividing the total force $\int_{S\times L} f_{em}(\mathbf{r}, V)\,d^3r$ by S (approximation of solid operating substance) with the subtraction of the hydraulic losses in the channel itself

$$P=\frac{1}{S}\int_{S\times L} d^3r f_{em}(\mathbf{r}, V) - \lambda\frac{L}{\delta_h}\frac{\varrho V^2}{2}\operatorname{sign} V. \quad (1)$$

For MHD machines a nonuniform distribution of the electromagnetic forces over the cross section of the channel is typical. In a number of cases the consequent inhomogeneity of the flow can be taken into consideration rigorously by joint solution of Navier–Stokes and Maxwell's equations. As an example the velocity distribution in laminar flow in a channel without lateral shorting strips is shown in Fig. 1, which is constructed from the data of [1]. In this case the electromagnetic force decreases around the side walls due to the transverse end effect. Here the pressure difference between the inlet and exit of the pump causes development of counterflow.

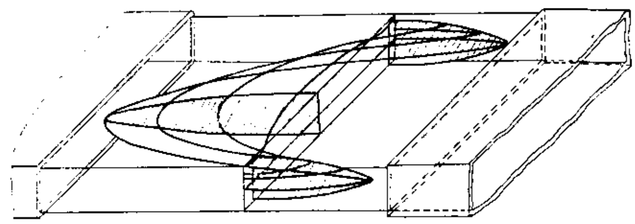

Fig. 1. Velocity distribution in laminar flow in a channel without side strips.

Translated from Magnitnaya Gidrodinamika, No. 1, pp. 87-101, January-March, 1975. Original article submitted November 15, 1974.

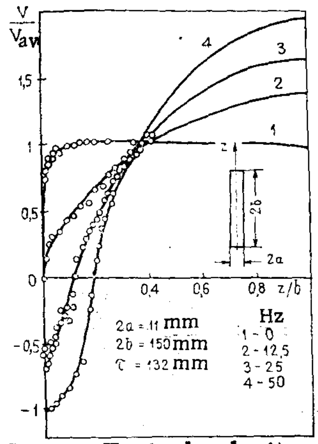

Fig. 2. Typical velocity profiles measured in a channel without side strips for constant discharge and current and for different values of frequency and counterpressure.

In most machines the cross section $S = l \times \delta_h$ is highly compressed in form $l \gg \delta_h$. For the investigation of a real turbulent flow in such channels we had proposed [2] that the hydraulic drag term in (1) be retained up to quadratic just as in the absence of the magnetic field, but the channel itself be divided imaginarily along the width into a large (in the limit infinite) number of elementary channels. These channels are connected in parallel (along the direction of flow of the fluid) hydraulically and in series (along the direction of the magnetizing current flow) electrically. Equation (1) is applied to each elementary channel separately and not to the machine as a whole. The pressure drop in all the elementary channels is the same, but in general f_{em} changes from channel to channel and (1) is an equation for determining V in each individual channel. Thus the variation of the velocity along the width l is taken into consideration explicitly and the velocity remains averaged only along the thickness δ_h. The total discharge is obtained by a summation (integration) of the discharges over all the elementary channels, $Q = \sum_i V_i S_i$.

The effectiveness of introducing this equivalent scheme of the MHD machine channel has been verified by a number of investigations devoted to the study of the characteristics of an induction pump with a channel without side strips. In [2] the regime of large slips ($s \approx 1$) is investigated, where the simplifying fact is that f_{em} is a function of only the coordinates and not of the local velocity. In [2] P(Q) characteristics, noticeably different from (1), as well as velocity distributions over the width of the channel, have been calculated. The next step was taken in [3] by taking the local values of the slip into consideration. The P(Q) characteristics thus computed agreed with the experiment much better than (1) [3, 4]. Direct measurements of the velocity distribution along the width of the channel of an actual pump were made at Leningrad Polytechnic Institute under the direction of Professor Tananaev. It was found that the velocity distribution has the form shown in Fig. 2 over most of the channel except the transition segments at the entrance and the exit.

This experiment provides a convincing argument that zones with very different velocities can exist within the channel of an MHD machine with a real turbulent regime.

In the present work a similar procedure is applied to a cylindrical MHD machine with arbitrary slips. In contrast to the plane pump without strips, where the electromagnetic forces are explicit functions of the coordinates, in a strictly symmetric machine there is no explicit dependence of the force on azimuth φ. In fact this is not so because of the implicit dependence of f_{em} on φ through $V(\varphi)$. In certain cases instability may appear, when the random deviations of the velocity from its mean generate in the force f_{em} an inhomogeneity that is sufficient to amplify the velocity deviations. After the development of the instability the operating section S is divided along the azimuth into several zones with very different (oppositely directed in pumps) velocities.

This instability is caused by the demagnetizing effect of the secondary currents flowing in the operating fluid and has some analogy with the stalling process of an ordinary asynchronous machine.

A complete investigation of the stability generally requires the discussion of the entire system, i.e., MHD machine + the external hydraulic circuit + the electric grid as a whole. In practice the problem is divided into several separate problems of different mathematical complexity. At first we shall consider mathematically simpler problems amenable to graphical interpretation. Systematic derivation of the conditions of internal instability and an example of computation of the inhomogeneous flow are given at the end of the article.

P(Q) Characteristics of an Ideal Cylindrical Machine

We consider a cylindrical machine (Fig. 3a) for which the magnetic gap δ_m between the central and external magnetic circuit is considerably smaller than both its radius R and the length of the pole division $\tau = \pi/\alpha$, i.e., $\delta_m \ll \min(R, \tau)$. The operating channel with hydraulic gap $\delta_h < \delta_m$ is placed in the magnetic gap. The linear current loading is a traveling wave

$$A(x, t) = \sqrt{2} A e^{i(\alpha x - \omega t)}. \tag{2}$$

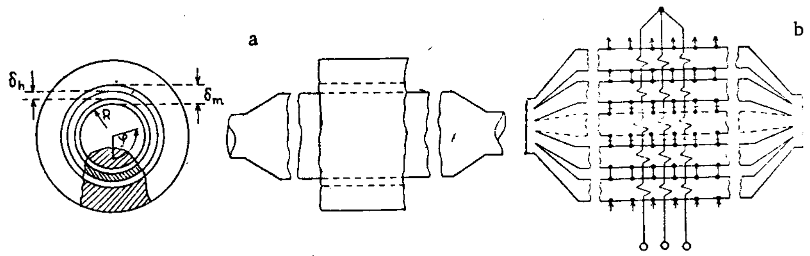

Fig. 3. Equivalent scheme of a cylindrical MHD machine: a large number of subchannels connected in parallel hydraulically and in series electrically.

The instability in question arises due to the fact that in the standard solid body approximation the P(Q) characteristic of the machine has a specific form. For the sake of consistency we give a simple derivation of it. In the simplest case both the magnetic field B and the density of the induced current $\sigma B(V-\omega/\alpha)$ are also traveling waves. The field is given by the equation

$$\frac{dB}{dx}=\mu_0\sigma\frac{\delta_h}{\delta_m}\left(V-\frac{\omega}{\alpha}\right)B+\frac{\sqrt{2}A\mu_0}{\delta_m}e^{i(\alpha x-\omega t)}, \tag{3}$$

from which we have

$$B=\frac{\sqrt{2}\mu_0 A e^{i(\alpha x-\omega t)}}{\alpha\delta_m[i-(V-\omega/\alpha)\mu_0\sigma\delta_h/\alpha\delta_m]} \tag{4}$$

and

$$f_{em}=\frac{-\mu_0^2\sigma A^2(V-\omega/\alpha)}{\delta_m^2\alpha^2[1+(V-\omega/\alpha)^2(\mu_0\sigma\delta_h/\alpha\delta_m)^2]}. \tag{5}$$

A substitution of (5) into (1) gives the well-known P(Q)-characteristic of the machine

$$P=-\frac{\mu_0\sigma A^2 L}{\delta_m^2\alpha^2}\frac{V-\omega/\alpha}{1+(V-\omega/\alpha)^2(\mu_0\sigma\delta_h/\alpha\delta_m)^2}-\lambda\frac{L}{\delta_h}\varrho\frac{V^2}{2}\operatorname{sign}V. \tag{6}$$

It is convenient to choose the following quantities as the scales of velocity, discharge, and pressure:

$$\text{synchronous velocity } V_0=\omega/\alpha,\quad \text{synchronous discharge } Q_0=2\pi R\delta_h V_0 \tag{7}$$

and hydraulic pressure losses in synchronous discharge

$$P_0=(L/\delta_h)\lambda\varrho V_0^2/2.$$

If we use the notation

$$p=P/P_0,\quad q=Q/Q_0, \tag{8), (9}$$

then (6) can be written in a considerably simpler form:

$$p=j^2\frac{1-q}{1+\varepsilon^2(1-q)^2}-q^2\operatorname{sign}q. \tag{10}$$

An example of the obtained characteristic is shown in Fig. 4.

Formula (10) contains two nondimensional parameters:

$$\varepsilon=\mu_0\sigma\omega\delta_h/\alpha^2\delta_m \tag{11}$$

and

$$j^2=2\mu_0^2\sigma A^2\delta_h/\lambda\varrho\alpha\omega\delta_m^2. \tag{12}$$

In the operation of an already constructed machine the quantity j may be regarded as nondimensional electric-supply current.

For $\varepsilon<1$ and small j^2 the entire p(q) characteristic is a monotonically decreasing one. But with the increase of j^2 growing segments with $(dp/dq>0)$ appear. At first this segment appears in the retarding

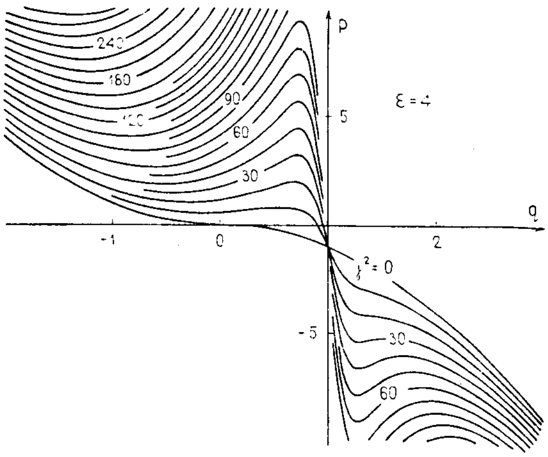

Fig. 4. Family of p(q) characteristics (10) with $\varepsilon = 4$ and given values of j^2.

region ($q < 0$) and later also in the generating region ($q > 1$). With the increase of ε the values of j necessary for the formation of these segments decrease. As soon as ε becomes greater than 1, the first segment from the retarding region extends partly also into the pump region ($0 < q < 1$). Formally this happens for all values of j. However, for small j the extension of this segment is small (in it the pressure difference is $\sim j^4$) and is noticeable only starting from $j \sim 1$. It can be shown that the growing segments of the p(q) characteristic are of practical significance in machines where the product

$$\varepsilon j^2 = \frac{2\mu_0{}^3\sigma^2\delta_h}{\lambda\varrho\alpha^3\delta_m{}^2}A^2 > \text{const.} \tag{13}$$

is sufficiently large.

Since the growing segments occur for $q < 1$ as well as for $q > 1$, the phenomena discussed below are almost identical in both regions. For the sake of definiteness henceforth everywhere below only one, i.e., the pump-retarding regime, is investigated unless stated otherwise; however, the same phenomena occur also in the region with negative slips.

Coupling of Single Ideal Pump with the External Hydraulic Circuit

The primary element of the investigated equivalent scheme (Fig. 3b) is the individual narrow pump, within which any velocity distributions are arbitrarily forbidden, i.e., it is a pump having characteristic (6). But the behavior of even such a pump in the hydraulic circuit can be specific.

With an external load the pump operates in steady state at the point of intersection of the P(Q) characteristic of the pump with the load:

$$P(Q)_{\text{pump}} = P(Q)_{\text{load}}. \tag{14}$$

The operating point (14) is stable if any random deviation of the discharge from its nominal value causes a pressure drop opposite to the deviation:

$$\frac{d}{dQ}[P(Q)_{\text{pump}} - P(Q)_{\text{load}}] < 0. \tag{15}$$

Different variants of stable (dark points) and unstable (light points) equilibrium are encountered depending on the nature of the load (Fig. 5).

A pump with characteristic (10) pumps the liquid across the quadratic resistance stably in the entire interval of control of resistance (Fig. 5a). Its regime is similar to the operation of an asynchronous motor in the scheme of Fig. 5b. The pumping of the liquid from one wide tank to another (Fig. 5c) is an example of the development of relaxation oscillations. As the tank on the right gets filled, the pressure drop at the pump increases. The operating point gets slowly displaced along the P(Q) characteristic of the pump from point A to C. At point C stability condition (15) is violated. Due to inertia the tank gets filled slightly above P_{max}. The pump is not in the state to hold the hydrostatic pressure and the liquid starts to get retarded. Simultaneously with Q the pressure developed by the tank also decreases. The liquid stops and begins to flow through the pump in the opposite direction. The pump stops and the operating point gets to point D. The entire transition of the operating point from C to D occurs considerably faster than the quasi-stationary motion from A to C; therefore it may be regarded as a unique jump. As the tank gets emptied the operating point slowly shifts from D to E. From here the operating point suddenly goes to point B along the horizontal [more precisely, along the P(Q) characteristic of the load] and then continues to move along the loop BCDE.

The instability of an MHD machine at point C is similar to the instability of an asynchronous motor going to stall. In the case of a passive load, which does not depend on the number of turns, the stalling of the motor gets completed by stopping (Fig. 5d). If we assume that a countermoment is applied to the axis

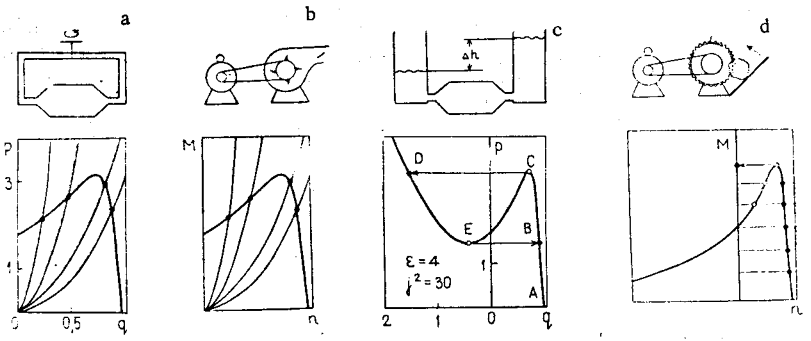

Fig. 5. Operation of pump and motor with different types of loads.

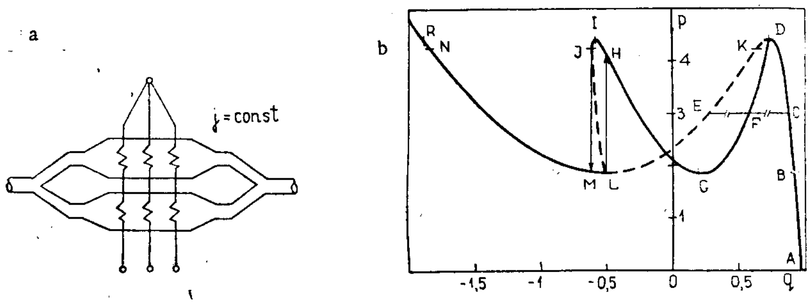

Fig. 6. Construction of the p(q) characteristic of a hydraulically parallel connection of two independent pumps in the regime j= const.

of the motor, that remains constant during the entire interval of change of the number of turns, then the analogy becomes more close.

There is a significant quantitative difference between the processes under consideration. The stalling of an asynchronous motor in these conditions occurs with an unwinding of the motor in the opposite direction to a very large number of rotations, since the braking moment caused by the friction in the bearings increases very slowly with the number of rotations. In contrast the resistance in an MHD machine increases as the square of the velocity. It is evident, for example, from Fig. 5d, that the stalling of the pump gets completed by its operation in the retarding regime with absolute value of the velocity of the same order as in the initial pump regime. This fact is significant for the subsequent discussion, since it provides a basis for considering the real coexistence of two zones with opposite velocities within a single channel. These zones may be formed due to the loss of stability from the homogeneous velocity distribution.

Simplest Composite Model of a Pump

The assumption that zones with different velocities are formed in the channel due to the loss of stability means that the elementary pumps of the equivalent scheme (see Fig. 3b) operate at different points of their P(Q) characteristics. A qualitative idea of the consequences of this assumption can be obtained by considering the simplest composite model of a pump containing two parallel, electrically independent subchannels.

Thus this model of the composite pump means a replacement of the equivalent scheme of Fig. 3b by the scheme of Fig. 6a with two identical ($j=j_1=j_2$, $\varepsilon=\varepsilon_1=\varepsilon_2$, $Q_{01}=Q_{02}$, $P_{01}=P_{02}$) elementary pumps. In parallel connection both develop the same pressure as the composite pump as a whole: $P=P_1=P_2$. The total discharge is the sum of the discharges of the two halves: $Q=Q_1+Q_2$. The synchronous discharges are also added up: $Q_0=2Q_{01}$. The hydrostatic pressure losses of the composite pump remain the same as for the parts: $P_0=P_{01}=P_{02}$. Therefore in terms of variables (8), (9) we have

$$p=p_1=p_2;\quad q={}^1/_2(q_1+q_2). \tag{16}$$

If it is stipulated that the discharges in both elementary pumps be equal, then the characteristic of the composite pump plotted in pq-coordinates must coincide with the characteristic of each elementary pump. This characteristic is shown in Fig. 6b by the line ABCDKELMNR.

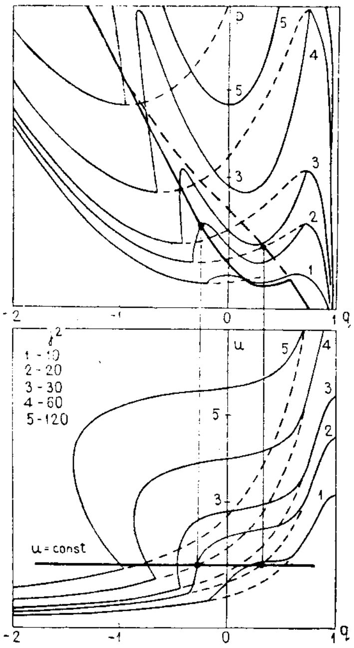

Fig. 7. Construction of p(q) characteristic for u = const.

However, the composite pump can operate even with nonequal discharges of the two elementary pumps. One half may be, for example, at point C and the other with the same pressure at E. According to (16) the operating point of the entire pump F must lie exactly at the midpoint of the segment CE. Choosing all possible operating points of each half and bisecting the segments connecting them, all the branches of the p(q) characteristic plotted in Fig. 6b can be constructed.

The stability of operation of the composite pump is determined by two conditions: a) the stability of the coupling with the external hydraulic circuit requires fulfillment of (15) for the resultant characteristic; b) the stability of the distribution of the total discharge Q between both halves is ensured by the second condition

$$\frac{d}{dQ_1}[P_1(Q_1)-P_2(Q-Q_1)]<0. \tag{17}$$

Condition (17) is not satisfied on two arcs DKEL and JL indicated by the dashed lines in Fig. 6b. Let us trace the displacement of the operating points on this figure as the discharge q decreases. For brevity we shall call the operating points of the two halves and of the entire pump the first, second, and resultant points. For p = 0 all the three points lie at A, after which all follow the arc ABCD together. At point D condition (17) breaks down and the discharges of the two halves are different ($q_1 \neq q_2$). Only one point (the first for definiteness) moves along DKL; the second moves in the opposite direction along DB, i.e., q_2 increases while q_1 decreases. The resultant point describes the arc DFG. When the first point reaches L, the second is at B and the resultant at G. Along the arc D to L the first goes into retardation ($q_1 < 0$). Further on the first point moves from L to R, the second from B to D, and the resultant from G to I. After this the second goes over to DK, the first goes from R back to N, and the resultant from I to J.

At the points N and K the slopes of the p(q) characteristics are equal but of opposite sign. Here both (15) for the resultant point and (17) break down simultaneously. Discharges q_1 and q_2 are equalized rather rapidly and the first and second points from N and K go to M. The resultant point also gets here with a jump from point J. Later all three points follow the arc MNR together. Thus on decreasing q the resultant point describes a complex path ABCDFGHIJMNR. On increasing q it goes over the reverse path along a somewhat different route RNMLHGFDCBA and the hysteresis loop JMLH appears as a result.

The above construction is a more complicated variant of the well-known academic problem about the behavior of two asynchronous motors driving a common shaft through a reducer of the type of an automobile differential. Such kinematically parallel motors retain identical rotations as long as both operate on the descending segments of the force characteristics. When attempt is made to take them to the ascending branch, only one of them gets there. The resultant characteristic is significantly worse compared to the case, when the differential is locked.

So far all the p(q) characteristics have been discussed in conditions of constant supply current j = const; in practice most pumps operate from a grid of stable voltage u = const. The difference between the regimes with j = const and u = const is determined by the ratio between the ohmic resistance of the winding R and the inductive impedance Z. Let us consider the limiting case $R \ll Z$, which is close to the case of operation of most pumps. In the solid-body approximation we have

$$Z \sim [i+\varepsilon(q-1)]^{-1} \tag{18}$$

[impedance proportional to field (4)]; considering the equality $u = |Z|\,j$, in the conditions u = const this relation leads to the decreasing p(q) characteristic

$$p = u^2(1-q) - q^2 \operatorname{sign} q. \tag{19}$$

The situation is more complex in the model of the composite pump. The two elementary pumps are electrically in series and their complex impedances are added up according to the law of addition of impedances:

$$Z \sim [i+\varepsilon(q_1-1)]^{-1} + [i+\varepsilon(q_2-1)]^{-1}. \tag{20}$$

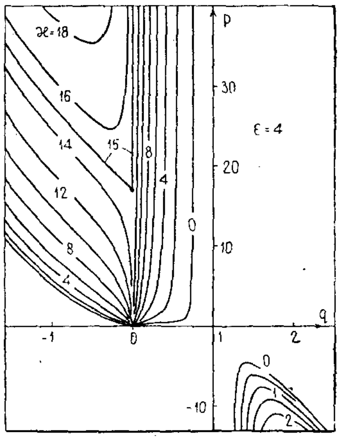

Fig. 8. Instability boundaries of a homogeneous flow in machines of different widths.

A graphical construction can be used for obtaining the dependence p(q) for u = const (Fig. 7). First a family of characteristics for different j = const is constructed by the method of Fig. 6b. The corresponding dependence u(q) for each of these curves is then constructed using formulas (20) and u = |Z| j. The desired p(q) characteristic is the graphical mapping of the straight line u = const from the plane uq to the plane pq. The characteristic thus obtained is shown by the heavy line in Fig. 7; the characteristic computed from formula (19) is shown by the dashed heavy line.

It is evident from Fig. 7 that in the regime u = const, just as in the regime j = const, there is a range of discharges, where the equal distribution of the flow between the pumps is unstable. The actual p(q) characteristic corresponding to unequal discharges turns out to be nonmonotonic and too low.

There are two unstable segments JL and DKEL on the p(q) characteristic with j = const (Fig. 6b). The variation of the electric supply stabilizes JL and in Fig. 7 a stable segment of the curve is obtained from it. The second segment (DKEL) corresponds to equal discharges in the two pumps. It turns out that the transition to the regime u = const does not stabilize the equal distribution of discharges between the pumps, i.e., an unstable segment (heavy dashed line) corresponds to DKEL even in conditions u = const. This is accounted for by the in-series connection of the pumps electrically. The discharges are equal on the arc DKEL: $Q_1 = Q_2 = Q/2$ and according to (20) small variations of the discharges δQ_1 and δQ_2 change the impedance by the amount

$$\delta Z \sim -\frac{2\varepsilon(\delta Q_1+\delta Q_2)}{Q_0[i+\varepsilon(q-1)]^2}, \tag{21}$$

proportional to the change of the total discharge $\delta Q_1 + \delta Q_2$. The instability in question develops in conditions, when the total discharge is conserved according to (16): $\delta Q_1 + \delta Q_2 = 0$. This means that the impedance Z does not change and the mode of electric supply can actually have no effect.

This last statement is of a more general nature than the composite pump model itself. Formula (21) is easily generalized to any arbitrary number of parallel pumps and does not change with the inclusion of the electrical connection of the pumps. This means that even in the exact formulation the boundary between stable and unstable homogeneous flows in the pq-plane forms a common curve for all modes of electric supply. Of course, the form of the p(q) characteristics themselves for homogeneous as well as inhomogeneous flow depends on the mode of supply: one characteristic for j = const, another for u = const, and still another for any intermediate regime. Whatever the characteristic is on which the pumps operate, the homogeneous velocity distribution loses stability at the point of intersection of this characteristic with the common stability boundary.

The regime j = const has a distinct place only for formal reasons. The elementary pumps are electrically in series and all are fed by the same current. Therefore it is convenient to fix just the current from which all the pumps get to operate on a single curve, and this considerably simplifies the investigation.

Boundary of Instability of Inhomogeneous Flow

The separation of the machine into two equal parts and disregard of the electrical contact between the elementary channels is a very rough approximation of the equivalent scheme in Fig. 3b. The present section of the article is devoted to a more consistent derivation of the stability conditions of homogeneous flow in a cylindrical machine.

As before we consider an MHD machine (see Fig. 3a), for which the linear current load represents a wave traveling along its axis. The longitudinal end effect is disregarded. The assumptions regarding the dimensions of the machine are the same: $\tau \ll L$, $\delta_h < \delta_m \ll \min(R, \tau)$. The main difference from the standard investigation lies in the fact that arbitrary azimuth dependence is allowed for the local value of the velocity and the amplitude of the magnetic field:

$$V(r,t) = V(\varphi); \quad B(r,t) = B(\varphi)e^{i(\alpha x - \omega t)}. \tag{22}$$

For determining $V(\varphi)$ and $B(\varphi)$ we have the equations

$$\left\{\frac{d^2}{R^2 d\varphi^2}-\alpha^2\left[1-i\varepsilon\left(1-\frac{V(\varphi)}{V_0}\right)\right]\right\}B(\varphi)=\frac{\sqrt{2}i\mu_0\alpha A}{\delta_m},$$

$$\frac{P}{L}=\frac{A}{\sqrt{2}\delta_h}\,\Re e\,B(\varphi)-\frac{\lambda\varrho V^2(\varphi)}{2\delta_h}\,\mathrm{sign}\,V(\varphi). \qquad (23)$$

If we introduce the additional notation

$$v(\varphi)=\frac{V(\varphi)}{V_0};\quad b(\varphi)=\frac{B(\varphi)\,\delta_m\alpha}{\sqrt{2}\mu_0 A};\quad \varkappa=\frac{1}{\alpha^2R^2}, \qquad (24)$$

we get the following system of nondimensional equations:

$$\left[\varkappa\frac{d^2}{d\varphi^2}-1+i\varepsilon(1-v(\varphi))\right]b(\varphi)=i; \qquad (25)$$

$$p=j^2\varepsilon^{-1}\,\Re e\,b(\varphi)-v^2(\varphi)\,\mathrm{sign}\,v(\varphi). \qquad (26)$$

Equations (25), (26) contain four dimensionless parameters: ε, $\varkappa$, p, and j. For all values of these parameters the system has the axisymmetric solution

$$v(\varphi)=q;\quad b(\varphi)=b_c=[i+\varepsilon(1-q)]^{-1}. \qquad (27)$$

The substitution of (27) into (26) gives the p(q) characteristic of the ideal machine, discussed above, corresponding to the uniform distribution of the velocity and the induction along the azimuth.

It can be shown that in a certain region of values of q, ε, $\varkappa$, and p or j Eqs. (25), (26) have other solutions besides (27); in view of this axisymmetric solution (27) is unstable.

Using the standard method of investigating stability we compute those values of discharge $q = q_m$, for which Eqs. (25), (26) have also the following solution besides (27):

$$v(\varphi)=q_m+\delta v_m\cos m\varphi;\quad b(\varphi)=b_c+\delta b_m\cos m\varphi \qquad (28)$$

with $$m=1,\ 2,\ 3\ldots;\quad |\delta v_m|\ll 1;\quad |\delta b_m|\ll|b_c|.$$

The presence of solutions (28) means that for $q = q_m$ small perturbations $\delta v_m \cos m\varphi$ of random origin do not change with time, i.e., they neither grow nor die out. The critical discharge q_m represents the boundary between the discharges, where the homogeneous flow is stable (to perturbations (28)), and discharges, where it is clearly unstable. It is assumed here that instabilities oscillating in time do not emerge from the more complicated temporal equations. The presence of the latter enlarges the region of instability.

The substitution of (28) into (25), (26) after linearization leads to the equation

$$[-m^2\varkappa-1+i\varepsilon(1-q_m)]\,\delta b_m=i\varepsilon b_c\delta v_m;$$
$$j^2\,\Re e\,\delta b_m=2\varepsilon|q_m|\,\delta v_m. \qquad (29)$$

The determinant of system (29) serves as the equation for q_m:

$$2|q_m|\,[\varepsilon^2(1-q_m)^2+1]\,[\varepsilon^2(1-q_m)^2+(1+m^2\varkappa)^2]-j^2[\varepsilon^2(1-q_m)^2-m^2\varkappa-1]=0. \qquad (30)$$

Solving (30) for q_m the critical discharges q_m can be in principle expressed as functions of j^2. Computing p from (25) the boundary of stability in plane pq can be drawn. In practice Eq. (30), which is a fifth-degree equation in q_m, presents some difficulties and can not be solved algebraically. Therefore it is more convenient to specify the value of the discharge and calculate the critical value of the pressure. For this purpose it is sufficient to eliminate j^2 from (30) with the use of (10) and write the result in the form

$$p_m=\frac{2|q|\,(1-q)\,[\varepsilon^2(1-q)^2+(1+\varkappa m^2)^2]}{\varepsilon^2(1-q)^2-1-\varkappa m^2}-q|q| \qquad (31)$$

with the additional condition

$$\varepsilon^2(1-q)^2-1-\varkappa m^2>0. \qquad (32)$$

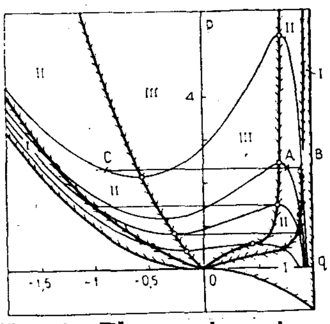

Fig. 9. Flow regimes in a wide pump: in region I the flow is clearly homogeneous, in III clearly inhomogeneous; in region II both regimes can exist.

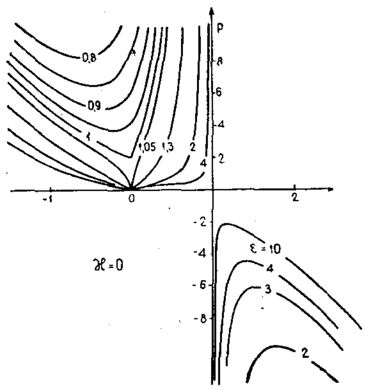

Fig. 10. Dependence of the boundary of clearly homogeneous flow on ε in wide machines.

The boundaries of instability computed from (31), (32) for different $\varkappa$ and for $\varepsilon = 4$ and $m = 1$ are shown in Fig. 8 as an example. Plotting similar curves for other values of ε and m it is possible to find a number of characteristic features. Thus the instability boundaries are always determined by the perturbations with $m = 1$. The instability corresponding to $m = 2, 3, 4, \ldots$ appears for such values of p and q, where the homogeneous flow is already unstable for $m = 1$. There are two instability regions in the pq plane: one for positive slips $(q < 1)$, i.e., in the pump-retardation regime, the other for negative slips $(q > 1)$. The instability region increases monotonically with $|p|$. For $|p| \to \infty$ the branches of the boundary closest to the synchronous discharge $(q = 1)$ have the asymptotes

$$q \to 1 \pm \varepsilon^{-1}(1+\varkappa)^{1/2}. \qquad (33)$$

When $\varepsilon^2 = 1 + \varkappa$, one branch coincides with the axis $q = 0$ and for $\varepsilon^2 < 1 + \varkappa$ the entire instability region $(q < 1)$ lies in the retardation part of the pq-plane. For $\varepsilon^2 > 1 + \varkappa$ the instability boundary passes through the coordinate origin $p = q = 0$, while for $\varepsilon^2 \leq 1 + \varkappa$ it does not reach the axis $p = 0$.

The effect of the ratio $\varkappa = (\tau/\pi R)^2$ on the stability has a simple qualitative explanation. A homogeneous flow induces homogeneous currents in the liquid. They form current circles of length $2\pi R$ around the machine. Any disturbance of the homogeneity of the flow disturbs also the current pattern. The inhomogeneous part of the currents can be closed only by making an additional path $\sim \tau$ along the pump. With the increase in $\varkappa$ the lengthening of the current lines becomes increasingly disadvantageous and the stability increases, as is evident from Fig. 8.

From the point of view of practical use small values of $\varkappa \leqslant 1$ are of greatest interest, which correspond to $R/\tau \geqslant 0.3$. It turns out that here $\varkappa$ has a relatively weak effect on the position of the stability boundary. In view of this the limiting case of wide pump $(\varkappa = 0)$ becomes of special interest. For the stability boundary we get the simple expression

$$p = \frac{2|q|(1-q)[\varepsilon^2(1-q)^2+1]}{\varepsilon^2(1-q)^2-1} - q|q| \qquad (34)$$

with the condition

$$\varepsilon^2(1-q)^2 > 1.$$

Boundary (34) passes through the extrema of the p(q) characteristics with $j = \text{const}$; in Fig. 9 it delineates region III, where the homogeneous flow is stable to small perturbations (absolutely unstable). Here only inhomogeneous flow can exist as a continuation. Using the family of p(q) characteristics with $j = \text{const}$ the other boundary, i.e., the boundary of absolute stability (Fig. 10), also can be constructed in the pq-plane of the wide pump. For this purpose a horizontal line should be drawn from each extremum (open dots) up to the intersection of the adjacent branch of the same characteristic. The set of all intersections (heavy dots) form the boundary between regions II and I. Both homogeneous and inhomogeneous flows can exist in region II. For example, the pump can operate at point A homogeneously for any single supply current. However, for another supply current it may turn out that a part of the cross section of the pump operates at point B, while the other part operates at C, and the widths of the two zones may be so chosen that the pump as a whole is again at point A. Perturbations of finite magnitude are required for taking the pump from one regime to another. In region I the separation of the flow into zones is impossible and here the homogeneous flow is absolutely stable.

The family of boundaries of absolute instability is shown in Fig. 10 for several values of ε.

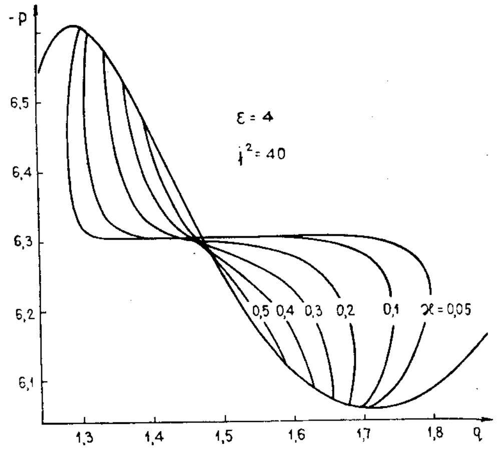

Fig. 11. The p(q) characteristics of machines with different width in the region of negative slips.

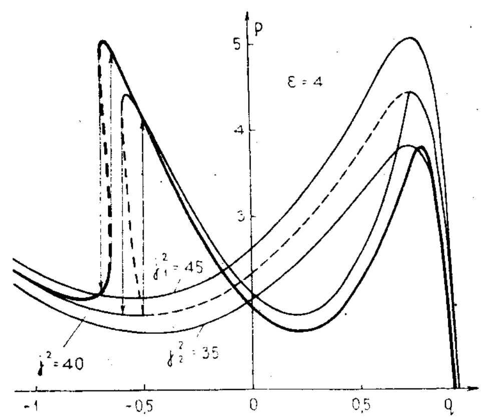

Fig. 12. Effect of asymmetry in the simplest model of a composite pump.

Example of Computation of p(q) Characteristic in the Presence of Inhomogeneous Flow

For those values of the discharge, where homogeneous regime (27) is unstable, Eqs. (25), (26) must have at least one stable solution that depends on φ. The unstable segment of the p(q) characteristic must be closed by another stable segment.

The closing arc can be computed, at least in principle, by a numerical integration of the system of equations (25), (26). However, the form of the closing arc may be subjected to strong perturbations from different operating factors that are difficult to control and are not taken into consideration in (25), (26). Therefore here we do not undertake the task of detailed computation of different cases of practical interest and give only one example from the region of negative slips. Here the computation is somewhat simpler than in the pump-retardation regime, where the factor sign (v) introduces an additional nonlinearity. The regime of stable current j = const is computed.

An approximate solution of (25), (26) was sought in the form of truncated Fourier series:

$$v(\varphi)\approx q+\sum_{n=1}^{N}\alpha_n\cos n\varphi;\quad b(\varphi)\approx b_0+\sum_{n=1}^{N}a_n\cos n\varphi. \tag{35}$$

The coefficients q, α_n, b_0, a_n were determined by the nonlinear system of algebraic equations

$$\begin{aligned} &p=j^2\varepsilon^{-1}\,\Re e\, b_0-\operatorname{sign} q\left(q^2+\frac{1}{2}\sum_{n=1}^{N}\alpha_n^2\right);\\ &[\varepsilon(1-q)+i]b_0=1+\frac{\varepsilon}{2}\sum_{n=1}^{N}a_n\alpha_n;\\ &j^2\varepsilon^{-1}\operatorname{sign} q\,\Re e\, a_n-2q\alpha_n=\frac{1}{2}\sum_{m=1}^{n-1}\alpha_m\alpha_{n-m}+\sum_{m=1}^{N-n}\alpha_m\alpha_{n+m};\\ &[\varepsilon(1-q)+i(1+n^2\varkappa)]a_n+\varepsilon b_0\alpha_n=\\ &=\frac{\varepsilon}{2}\left\{\sum_{m=1}^{n-1}a_m\alpha_{n-m}+\sum_{m=1}^{N-n}(a_m\alpha_{n+m}+a_m\alpha_{n+m})\right\}, \end{aligned} \tag{36}$$

obtained directly by substituting (35) into (25), (26). The solution of system (36) was obtained numerically on a computer. The computed p(q) characteristics with $\varepsilon = 4$, $j^2 = 40$ are shown in Fig. 11 for different values of the nondimensional width $\varkappa^{-1/2}$. The ends of the unstable segment of the p(q) characteristic are actually connected by an arc which is similar to the corresponding arc in the simplest model of the composite machine (see Fig. 6). We note, however, that there are also a number of qualitative differences. A parallel connection of two identical machines loses stability at the extremums of the homogeneous p(q) characteristic. For finite values of $\varkappa$ the closing arc departs from the homogeneous characteristic at points located between the extrema due to narrowing of the instability region. Furthermore, in Fig. 6 one end of the connecting arc has positive slope and the other has negative slope; in Fig. 11 the slope of the end of this arc depends also on $\varkappa$. It is found that the transition from the homogeneous to the inhomogeneous regime and back, caused by the change in q, occurs smoothly only for sufficiently large values of $\varkappa$.

In the example discussed above the parameters of the machine were chosen only from considerations of the economy of computer time. The values $\varepsilon = 4$ and $j^2 = 40$ were taken from the region of weak nonlinearity, where series (35) could be restricted to a small number of terms (for large $\varkappa$ it was sufficient to take N = 3; with the decrease in $\varkappa$ N had to be gradually increased to 6). This simplified the computation and the pattern could be obtained, even though it was not the most typical.

On Phenomena in Real Machines

In the investigation of the flow in real machines a number of important factors that have been disregarded in the theory discussed above have to be taken into consideration. These factors can be arbitrarily divided into two groups changing the phenomenon qualitatively or only quantitatively.

An example of the first group is the almost unavoidable small asymmetry of the machine caused by imperfection in construction. In order to see the effect of the asymmetry the same graphs as in Fig. 6 are plotted in Fig. 12, but for a model consisting of two slightly different pumps. As an example the current j was varied, but ε or both parameters together could be varied with the same result. The characteristic of the symmetric model is also plotted for comparison. It is found that the asymmetry leads to three basic consequences: a) the sharp angles are rounded off; b) the area of the hysteresis loop decreases (for large asymmetry the loop disappears); c) the remaining elements of the curve are somewhat deformed. The effect of the asymmetry appears primarily at or close to those discharges, for which the instability of the homogeneous flow is observed.

The asymmetry is not a unique constantly acting perturbation; the turbulent nature of the flow also comes into play here. Velocity perturbations (mainly longitudinal) must also lead to rounding off of the angles of the characteristics and to a narrowing (if not closing) of the hysteresis loop.

Of the second group of factors the longitudinal end effect should be mentioned. The finite length of the machine may appreciably delay the onset of the instability. The transverse oscillations of the velocity transferring momentum along the azimuth may also lead to the same result.

For these reasons smoother p(q) characteristics than in Fig. 11 should be expected for real machines. However, the statement that in the region of multivelocity flow these characteristics still must be shifted relative to the computed ones, remains valid.

The phenomena described here should be regarded undesirable. As far as possible MHD machines should not be operated in regions where the multivelocity regime may potentially exist (region II in Fig. 9), or in any case in regions where the homogeneous flow is unstable (region I in Fig. 9). Special attention must be given to the stabilization of the hydrodynamic regime.

LITERATURE CITED

1. R. A. Petrovicha and L. Ya. Ulmanis, Papers Presented at the Fourth Tallin Conference on Electromagnetic Flowmeters [in Russian], Vol. II, No. III, Tallin (1969).
2. A. Gailitis and O. Lielausis, Magnitn. Gidrodinam., No. 2, 123 (1971).
3. A. Ya. Kalnin', Ch. K. Mikryukov, R. A. Petrovicha, V. A. Rupeneit, and L. Ya. Ulmanis, Magnitn. Gidrodinam., No. 4, 94 (1971).
4. S. V. Vasil'ev, R. A. Petrovicha, and V. A. Rupeneit, Magnitn. Gidrodinam., No. 4, 150 (1973).